Appendix C. Nomenclature – alternative terms

Name	Alternative term
Accessory lung lobe	Azygos lung lobe Caudate lung lobe Medial lobe Post-caval lung lobe
Anterior vena cava	Cranial vena cava Superior vena cava
Calcaneus	Calcaneum
Cervical vertebra 1	Atlas
Cervical vertebra 2	Axis
Exoccipital	Occipital condyle
Forepaw digit 1	Pollex
Hindpaw digit 1	Hallux
Incisor socket	Incisor alveolus
Liver – papillary process (rabbit)	Quadrate lobe Caudate lobe
Odontoid process	Dens
Orbita	Orbital socket
Palatine rugae	Palatine ridges
Posterior vena cava	Caudal vena cava Inferior vena cava
Premaxilla	Incisive
Rib cartilage	Costal cartilage
Ribs attached to sternum (numbers 1–7 in rats, mice and rabbits)	True ribs (vertebrosternal ribs)
Ribs with long rib cartilages but not attached to sternum (usually numbers 8–10 in rats, mice and rabbits)	False ribs
Ribs with short costal cartilages, not attached to sternum (usually numbers 11–12/13 in rats, mice and rabbits)	Floating false ribs
Squamosal	Squamous temporal Temporal
Sternebra 1	Manubrium
Sternebra 6	Xiphisternum
Talus	Astragalus
Tympanic annulus	Tympanic arch Tympanic ring
Ventral portion of cervical vertebra 1	Ventral arch
Vertebral arch	Dorsal arch Neural arch
Vertebral canal	Spinal canal
Vertebral centrum	Vertebral body
Zygomatic	Jugal Malar Zygoma

Appendix D. Structural differences – rat, mouse and rabbit

Structure	Rat	Mouse	Rabbit
Azygos vein (dorsal thorax, close to midline)	Left side	Left side	Right side
Umbilical artery (alongside urinary bladder)	Right side	Right side	Bilateral
Lung lobes	Left lobe	Left lobe	Left lobe, subdivided into: – left cranial lobe – left caudal lobe
	Right lobe, subdivided into: – right cranial lobe – right middle lobe – right caudal lobe – accessory lobe[a]	Right lobe, subdivided into: – right cranial lobe – right middle lobe – right caudal lobe – accessory lobe[a]	Right lobe, subdivided into: – right cranial lobe – right middle lobe – right caudal lobe – accessory lobe[a]
Liver lobes	Left lobe, subdivided into: – left medial lobe – left lateral lobe	Left lobe, subdivided into: – left medial lobe – left lateral lobe	Left lobe, subdivided into: – left medial lobe – left lateral lobe
	Right lobe, subdivided into: – right medial lobe – right lateral lobe – papillary process (cranial and caudal to stomach) – caudate process	Right lobe, subdivided into: – right medial lobe – right lateral lobe – papillary process (cranial and caudal to stomach) – caudate process	Right lobe, subdivided into: – right medial lobe – right lateral lobe including papillary process[a] (cranial to stomach) and caudate process (projecting dorsally towards right kidney)
Gall bladder	Not present; however a bile duct is present.	Present	Present

Appendix D (*Continued*)

Structure	Rat	Mouse	Rabbit
Cervical vertebrae[b]	7	7	7
Thoracic vertebrae[b]	13	13	12 or 13
Ribs (excluding supernumerary)	13	13	12 or 13
– true (articulated with sternum)	7	7	7
– false (long costal cartilage, but not articulated with sternum)	3	3	3
– floating false (short costal cartilage, and not articulated with sternum)	3	3	2 or 3
Lumbar vertebrae[b]	6	6	6 or 7
Sacral vertebrae	4	4	4
Caudal vertebrae	Variable – approx 27	Variable – approx 27	Variable – approx 19

[a] See Appendix C for alternative names.
[b] See also Fig. 1 – Typical vertebral configurations in rodents and rabbits.

Appendix E. Commonly observed skeletal foramina and processes

	FORAMINA	
	Bone	Foramen
Mandible		Mental foramen
Maxilla		Infra-orbital foramen
		Rostral (anterior) palatine foramen
Occipital	Supra-occipital/exoccipitals/basio-occipital	Foramen magnum
	Exoccipital	Hypoglossal canal
Premaxilla (incisive)		Rostral (anterior) palatine foramen[a]
Sphenoid	Basisphenoid	Craniopharyngeal canal
	Presphenoid/orbitosphenoid	Optic foramen
Vertebra	Cervical arches 1–6	Transverse foramina (vertebrateral canals)

	PROCESSES	
	Bone	Process
Frontal		Orbital process
		Rostral supra-orbital process[b]
		Caudal supra-orbital process[b]
Mandible		Dental ridge/process
		Coronoid process
		Condylar (condyloid) process
		Angular process (angle)
Maxilla		Dental (alveolar) process
		Orbital process
		Palatine process
		Zygomatic process
Premaxilla (incisive)		Nasofrontal process
		Palatine process
Sphenoid	Basisphenoid	Pterygoid process
	Presphenoid	Orbitosphenoid
Squamosal (Squamous temporal)		Retrotympanic process[c]
		Zygomatic process
Vertebra	Ventral arch of vertebra 1	Ventral tubercle
	Cervical centrum 2	Odontoid process
	Arch	Transverse process
		Neural spine (spinous process)
	Arches except cervical 1 (Atlas) and 2 (Axis)	Cranial articular process (prezygopophysis)
	Arches except cervical 1 (Atlas)	Caudal articular process (postzygopophysis)
	Cervical arch 6	Anterior tubercle (ventral plate, lamina ventralis)
	Lower thoracic and lumbar arches	Accessory process (anapophysis)
Rib		Tubercle
Scapula	Blade	Coracoid process
	Spine	Acromion process
		Metacromion process
Humerus		Deltoid tuberosity[d]
Ulna		Olecranon process

[a] Also known as Incisive foramen.
[b] Observed in the rabbit.
[c] Also known as Post-tympanic process or Retroarticularis process.
[d] Observed in the rat and mouse.

Human & Experimental Toxicology (2009) 28: 231–244
www.het.sagepub.com

Gene expression profiling in rat liver treated with compounds inducing elevation of bilirubin

M Hirode[1,2], A Horinouchi[1,2], T Uehara[2], A Ono[2,3], T Miyagishima[2], H Yamada[2], T Nagao[4], Y Ohno[2,3] and T Urushidani[2,5]

[1]Development Research Center, Pharmaceutical Research Division, Takeda Pharmaceutical Company Limited, Yodogawa-ku, Osaka, Japan; [2]Toxicogenomics Informatics Project, National Institute of Biomedical Innovation, Ibaraki, Osaka, Japan; [3]National Institute of Health Sciences, Setagaya-ku, Tokyo, Japan; [4]Food Safety Commission of Japan, Chiyoda-ku, Tokyo, Japan; and [5]Department of Pathophysiology, Doshisha Women's College of Liberal Arts, Kyotanabe, Kyoto, Japan

We have constructed a large-scale transcriptome database of rat liver treated with various drugs. In an effort to identify a biomarker for the diagnosis of elevated total bilirubin (TBIL) and direct bilirubin (DBIL), we extracted 59 probe sets of rat hepatic genes from the data for seven typical drugs, gemfibrozil, phalloidin, colchicine, bendazac, rifampicin, cyclosporine A, and chlorpromazine, which induced this phenotype from 3 to 28 days of repeated administration in the present study. Principal component analysis (PCA) using these probes clearly separated dose- and time-dependent clusters in the treated groups from their controls. Eighteen more drugs in the database, reported to elevate TBIL and DBIL, were estimated by PCA using these probe sets. Of these, 12 drugs, that is methapyrilene, thioacetamide, ticlopidine, ethinyl estradiol, alpha-naphthylisothiocyanate, indomethacin, methyltestosterone, penicillamine, allyl alcohol, aspirin, iproniazid, and isoniazid were also separated from the control clusters, as were the seven typical drugs causing elevation of TBIL and DBIL. The principal component 1 (PC1) value showed high correlation with TBIL and DBIL. In the cases of colchicine, bendazac, chlorpromazine, gemfibrozil, and phalloidin, the possible elevation of TBIL and DBIL could be predicted by expression of these genes 24 h after single administration. We conclude that these identified 59 probe sets could be useful to diagnose the cause of elevation of TBIL and DBIL, and that toxicogenomics would be a promising approach for prediction of this type of toxicity.

Key words: bilirubin; liver; principal component analysis; rat; toxicogenomics

Introduction

The Toxicogenomics Project is a 5-year collaborative project by the National Institute of Biomedical Innovation, the National Institute of Health Science, and 15 pharmaceutical companies in Japan that started in 2002.[1] Its aim was to construct a large-scale toxicology database of transcriptomes to predict toxicity of new chemical entities in the early stage of drug development. Over 150 chemicals, mainly medicinal compounds, were selected and their gene expression in the liver was comprehensively measured by using Affymetrix GeneChip®, Santa Clara, California, USA. In 2007, the project was finished and the whole system, consisting of the database, the analyzing system, and the prediction system, was completed and named as TG-GATEs (Genomics Assisted Toxicity Evaluation System developed by the Toxicogenomics Project, Japan). Recently, we identified a biomarker for the diagnosis of hepatic phospholipidosis, nongenotoxic hepatocarcinogenicity, glutathione depletion-responsive, and serum triglyceride-decreasing by using our database.[2–5]

Bilirubin is mainly a breakdown product of heme (part of the hemoglobin in the red blood cells). The heme is then turned into unconjugated bilirubin (indirect bilirubin) in the macrophages of the spleen. It is then bound to albumin and sent to the liver. In the liver it is conjugated with glucuronic acid (direct bilirubin, DBIL), making it soluble in water. Total bilirubin (TBIL) and DBIL levels can be measured in the blood, but indirect bilirubin is calculated from the

Correspondence to: Mitsuhiro Hirode, Development Research Center, Pharmaceutical Research Division, Takeda Pharmaceutical Company Limited, Yodogawa-ku, Osaka, 532-8686, Japan.
Email: Hirode_Mitsuhiro@takeda.co.jp

10.1177/0960327109104528

total and direct bilirubin. Bilirubin levels reflect the balance between production and excretion.

Increased TBIL causes jaundice of the prehepatic, hepatic, and posthepatic types. The "prehepatic type" is derived from increased bilirubin production. This can be due to a number of causes, including hemolytic anemia and internal hemorrhage. If the DBIL is normal, then the problem is an excess of unconjugated bilirubin, and the location of the problem is upstream of bilirubin excretion. The "hepatic type" indicates problems in the liver, which are reflected as deficiencies in bilirubin metabolism (e.g., reduced hepatocyte uptake of bilirubin, impaired conjugation of bilirubin, and reduced hepatocyte secretion of bilirubin). Some examples would be drug-induced hepatic disorders (especially antipsychotic drugs, some sex hormones, and a wide range of other drugs), cirrhosis, and viral hepatitis. The "posthepatic type" is derived from obstruction of the bile ducts, which are reflected as deficiencies in bilirubin excretion. An obstruction such as gallstones or cancer can be located either within the liver or outside the liver.

In the present study, we selected elevation of TBIL and DBIL as a target phenotype and tried to identify candidate biomarkers that identify chemicals with the potential to cause this phenotype by using our database.

Materials and methods

Compounds

The compounds used for the data analysis are listed in Table 1, in which the chemical name, abbreviation, dosage, administration route, and vehicle used in the study are summarized.

Animal treatment

The experiments were carried out as previously described in the literature.[6] Male Crl:CD (SD) rats were purchased from Charles River Japan Inc., (Kanagawa, Japan) at 5 weeks of age. After a 7-day quarantine and acclimatization period, the animals were divided into groups of five animals, using a computerized stratified random grouping method based on the body weight for each age. The animals were individually housed in stainless-steel cages in a room that was lighted for 12 h (7:00 a.m–7:00 p.m) daily, ventilated with an air-exchange rate of 15 times per hour, and maintained at 21–25 °C with a relative humidity

Table 1 List of compounds used in the present study

Compound name	*Abbreviation*	*Dose (dose level, mg/kg)*			*Administration route*	*Vehicle*	*Bilirubin*
		Low	*Middle*	*High*			
Gemfibrozil	GFZ	30	100	300	po	CO	A
Phalloidin	PHA	NA	NA	0.5	ip	SA	B
Colchicine	COL	1.5/0.5[a]	5/1.5[a]	15/5[a]	po	MC	C
Bendazac	BDZ	100/30[a]	300/100[a]	1000/300[a]	po	MC	C
Rifampicin	RIF	20	60	200	po	MC	C
Cyclosporine A	CSA	30/10[a]	100/30[a]	300/100[a]	po	CO	B
Chlorpromazine	CPZ	4.5	15	45 (150[b])	po	MC	C
Methapyrilene	MP	10	30	100	po	MC	B
Thioacetamide	TAA	4.5	15	45	po	MC	C
Ticlopidine	TCP	30	100	300	po	MC	D
Ethinyl estradiol	EE	1	3	10	po	CO	A
Alpha-naphthylisothiocyanate	ANIT	1.5	5	15	po	CO	D
Indomethacin	IM	0.5	1.6	5	po	MC	C
Methyltestosterone	MTS	30	100	300	po	MC	A
Penicillamine	PEN	100	300	1000	po	MC	A
Allyl alcohol	AA	3	10	30	po	CO	D
Aspirin	ASA	45	150	450	po	MC	D
Iproniazid	IPA	6	20	60	po	MC	B
Isoniazid	INAH	50	100	200	po	MC	C
Glibenclamide	GBC	100	300	1000	po	CO	D
Cyclophosphamide	CPA	1.5	5	15	po	MC	B
Nitrofurantoin	NFT	10	30	100	po	MC	D
Valproate	VPA	45	150	450	po	MC	D
Methotrexate	MTX	0.1	0.3	1	po	MC	C
Tetracycline	TC	100	300	1000	po	MC	C

po, peroral; CO, corn oil; A, bilirubin oxidase method; NA, not applicable; ip, intraperitoneal; SA, saline; B, vanadate oxidation method; MC, 0.5 wt/vol% methylcellulose; C, azobilirubin method; D, alkali azobilirubin method.
The animals were treated for 3, 7, 14, or 28 days, except PHA, which were treated for 3 or 7 days.
[a]As single dose/repeated dose.
[b]Extra-high dose (only single dose of CPZ).

of 40–70%. Each animal was allowed free access to water and pellet food (CRF-1, sterilized by radiation, Oriental Yeast Co., Tokyo, Japan). Rats in each group were orally dosed various drugs suspended or dissolved either in 0.5% methylcellulose solution or corn oil according to their dispersibility, except phalloidin, which was dissolved in saline and administered intraperitoneally. For single-dose experiments the rats were sacrificed at 3, 6, 9, and 24 h after dosing. For repeated dose experiments, the animals were treated for 3, 7, 14, or 28 days, except phalloidin, which were treated for 3 or 7 days, and they were sacrificed 24 h after the last dosing. Food was not withdrawn before sacrifice and the time of autopsy was done between 9:00 a.m–11:00 a.m. for the repeated dose group and 24 h after the single dose group. Blood samples for routine biochemical analysis were collected into heparinized tubes under ether anesthesia from the abdominal aorta after which the animals were sacrificed. As the animal experiments were performed in four different contract research organizations where different automated blood chemistry analyzers were used, TBIL and DBIL were quantified by four different methods, that is bilirubin oxidase method (TBA-120FR, Toshiba Medical Systems Corporation, Tokyo, Japan), vanadate oxidation method (Hitachi H7170, Hitachi High-Technologies Corporation, Tokyo, Japan), azobilirubin method (COBAS MIRA plus, Roche Diagnostics, Indianapolis, Indiana, USA), and alkali azobilirubin method (Hitachi H7070, Hitachi High-Technologies Corporation, Tokyo, Japan). Because of this difference, the absolute values could not be compared, and the judgment of hyperbilirubinemia was done based on the difference from the control value. These methods are shown in Table 1 as A, B, C, and D in this order. The experimental protocols were reviewed and approved by the Ethics Review Committee for Animal Experimentation of the National Institute of Health Sciences.

Microarray analysis

After collecting the blood the animals were euthanized by exsanguination from the abdominal aorta under ether anesthesia. An aliquot of the sample (about 30 mg) for RNA analysis was obtained from the left lateral lobe of the liver in each animal immediately after sacrifice, kept in RNAlater® (Ambion, Austin, Texas, USA) overnight at 4 °C, and frozen at −80 °C until use. Liver samples were homogenized with the buffer RNeasy Lysis Buffer (RLT) supplied in the RNeasy Mini Kit (Qiagen, Valencia, California, USA) and total RNA was isolated according to the manufacturer's instructions. Microarray analysis was conducted on three out of five samples, selected based on their body weight excluding the highest and the lowest, for each group by using the GeneChip® Rat Genome 230 2.0 Arrays (Affymetrix, Santa Clara, California, USA), containing 31,042 probe sets. The procedure was conducted basically according to the manufacturer's instructions using the Superscript Choice System (Invitrogen, Carlsbad, California, USA) and T7-(dT)24-oligonucleotide primer (Affymetrix) for cDNA synthesis, cDNA Cleanup Module (Affymetrix) for purification, and BioArray High yield RNA Transcript Labeling Kit (Enzo Diagnostics, Farmingdale, New York, USA) for synthesis of biotin-labeled cRNA. Ten micrograms of fragmented cRNA were hybridized to a Rat Genome 230 2.0 Array for 18 h at 45 °C at 60 rpm, after which the array was washed and stained by streptavidin-phycoerythrin using a Fluidics Station 400 (Affymetrix) and then scanned by a Gene Array Scanner (Affymetrix). The digital image files were processed by Affymetrix Microarray Suite version 5.0 Affymetrix, and intensities were normalized for each chip by setting the mean intensity to 500 (per chip normalization).

Microarray data analysis

To extract probe sets related to the elevation of TBIL and DBIL, we first used the gene expression data from liver from rats treated by repeated administration for 3, 7, 14, and 28 days, with gemfibrozil (GFZ), phalloidin (PHA), colchicine (COL), bendazac (BDZ), rifampicin (RIF), cyclosporine A (CSA) and chlorpromazine (CPZ), which are known to cause elevation of TBIL and DBIL, and that was confirmed in the present study.

After removing the probe sets with Affymetrix absent call in all the 48 sample sets ($N = 3$ for 4 time points and 4 dose levels for one drug), except PHA, which had 12 sample sets ($N = 3$ for 2 time points by repeated administration for 3 and 7 days, and 2 dose levels), genes differentially expressed by the treatment were extracted by Welch's ANOVA/*t*-test ($P < 0.05$) for the dose level at one time point. This procedure was continued for all time points, and the genes showing significant change at any point were combined as elevation of TBIL and DBIL responsive genes. In the next step, commonly mobilized genes among these seven chemicals were selected.

The individual expression value (global mean) was converted to ratio by the mean of corresponding control value, and all the values with different doses and time points of the test compounds were gathered, and they were normalized by converting them to *z*-scores for each gene (pergene normalization). Principal component analysis (PCA) was

performed using Spotfire Decision Site (Spotfire, Somerville, Massachusetts, USA).

Pathway and gene ontology (GO) analysis

The identified probe sets were subjected to GO analysis by DAVID (Database for Annotation, Visualization, and Integrated Discovery; http://david.abcc.ncifcrf.gov/) using Fisher's exact test.[7]

Results

Blood biochemical examination

The results of TBIL and DBIL examination of seven typical compounds (GFZ, PHA, COL, BDZ, RIF, CSA, and CPZ) known to induce their elevation in rat plasma are shown in Figure 1. In most cases, both TBIL and DBIL were elevated and this tended to progress with dose and time. In the cases of COL and BDZ, DBIL was increased with a peak at 4th day and TBIL showed the same change as COL. TBIL was increased for all sampling points at high dose of BDZ. With CPZ, the DBIL was elevated at the 15th day or later, but changes in the TBIL were obscure at any sampling point.

Microarray data analysis

Differentially expressed genes with statistically significant differences were extracted from each of the seven representative drugs elevating TBIL and DBIL as described in the Materials and methods section. The numbers of extracted probe sets were 3690 for

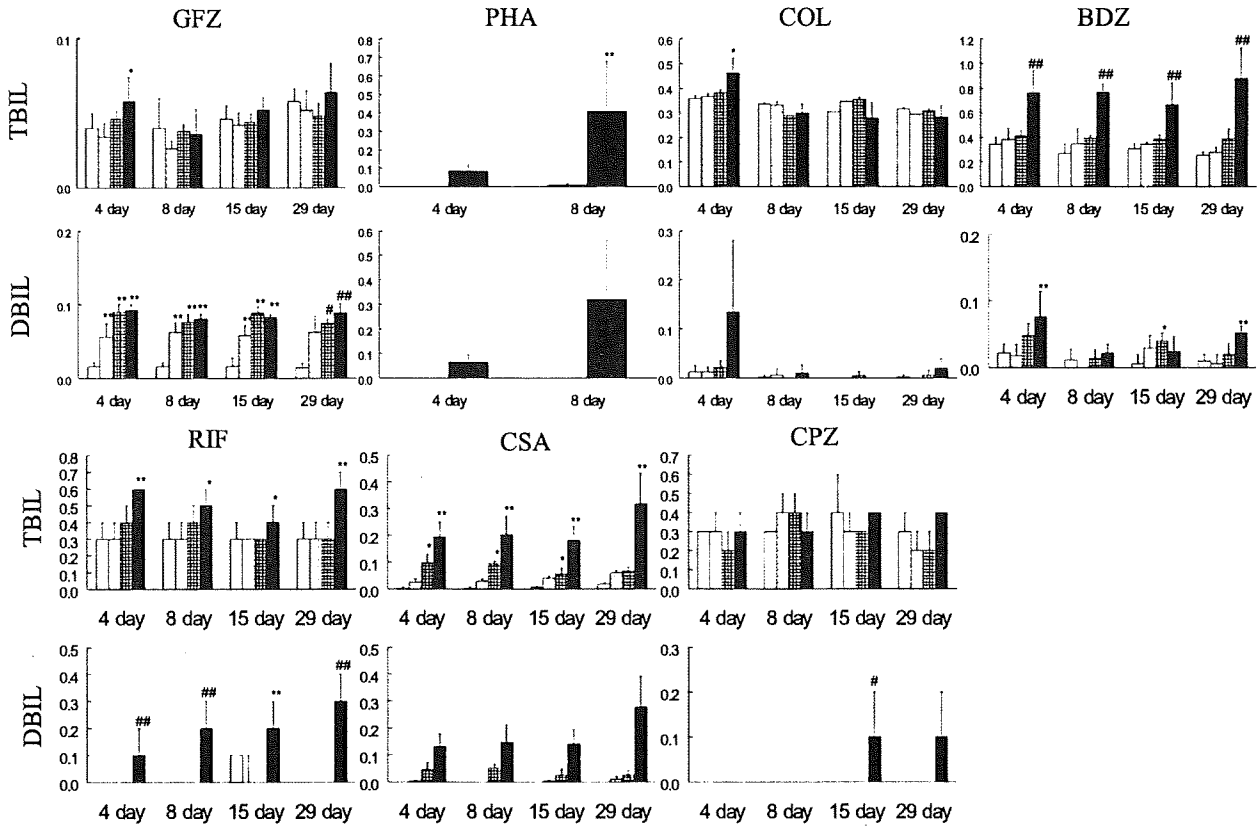

Figure 1 Plasma total bilirubin (TBIL) and direct bilirubin (DBIL) concentrations for rats treated with gemfibrozil (GFZ), phalloidin (PHA), colchicine (COL), bendazac (BDZ), rifampicin (RIF), cyclosporine A (CSA), or chlorpromazine (CPZ). Six-week-old male Sprague-Dawley rats were treated with each compound for 3, 7, 14, or 28 days, and they were sacrificed 24 h after the last dose. Blood samples were collected at sacrifice. Plasma TBIL and DBIL concentrations were estimated as described in the Materials and methods section. As the animal experiments were performed in four different contract research organizations where different automated blood chemistry analyzers were used, TBIL and DBIL were quantified by four different methods (see Table 1). Because of this difference, the absolute values could not be compared and the judgment of hyperbilirubinemia was done based on the difference from the control value. Open (control), dotted (low dose), checked (middle dose) and filled (high dose) columns represent plasma TBIL and DBIL concentrations (mg/dL). Values are expressed as mean ± SD of five rats each for each time and compound. Significant difference from the control rats: ($*P < 0.05$, $**P < 0.01$: Dunnett test, $\#P < 0.05$, $\#\#P < 0.01$: Dunnett type mean rank test).

BDZ, 5398 for COL, 3473 for CPZ, 4258 for CSA, 4656 for GFZ, 4917 for PHA, and 2403 for RIF. We then selected the probe sets that were commonly changed in all the compounds and 59 probe sets were obtained. A list of these probe sets is in Table 2, where each probe is categorized by its biological function. Figure 2 shows the expression changes of these 59 probe sets at high dose of repeated administration, as a heat map of the average of log 2 ratios. It appears that the trend of the change is to decrease, and the direction of change of the probe sets is not necessarily common with these drugs. Based on gene ontology, the contents of the genes related to cellular metabolism, biosynthesis, lipid metabolism, cellular biosynthesis, cellular physiological process, response to stress, physiological process, and serine family amino acid metabolism were significantly increased (Table 3).

Principal component analysis

Using the 59 probe sets extracted as above, PCA was performed on the seven drugs elevating TBIL and DBIL. As shown in Figure 3, the treated samples were dose-dependently separated to form clusters from the controls, mainly toward the direction of PC1 (contribution rate: 30.4%). Of the genes contributing to PC1, those with high eigenvalue are listed in Table 4. To examine the time-dependency, all the samples were aligned on a one dimensional graph of PC1 (Figure 4). It appeared that the PC1 value generally increased with time and with the dose for these drugs. In the cases of COL and BDZ, the PC1 value increased with the peak on the 4th day. In case of CPZ, time- and dose-dependency were obscure although the group treated clearly formed a cluster separated from the control cluster.

Verification of the probe sets using 18 test compounds

In a survey of the literature, in addition to the seven drugs above, we identified 18 more drugs in our database that had been reported to elevate TBIL and DBIL. The data of TBIL and DBIL of the 18 compounds are shown in Figure 5. We performed PCA using the 59 probe sets on the seven typical and 18 additional drugs (25 total), and depicted them in Figure 6 as a one-dimensional graph with PC1 (contribution rate: 35.9 %). It was revealed that 12 out of 18 drugs, that is methapyrilene, thioacetamide, ticlopidine, ethinyl estradiol, alpha-naphthylisothiocyanate, indomethacin, methyltestosterone, penicillamine, allyl alcohol, aspirin, iproniazid, and isoniazid were separated from control clusters in the same way as the seven typical drugs elevating TBIL and DBIL. Of these 12 drugs, MP, TAA, EE, ANIT, PEN, and IPA showed significant elevation of TBIL and DBIL for at least one time point during repeated administration, whereas the remaining six drugs did not show any toxicologically meaningful elevation. Glibenclamide (GBC) and cyclophosphamide did not change their position very much on the PCA, whereas their extent was roughly equivalent to that of CPZ, a positive control. The remaining four drugs, that is nitrofurantoin, valproate, methotrexate, and tetracycline stayed in the same position as their controls. Reviewing the data of TBIL and DBIL of the latter six drugs with low PC1 values, it was revealed that a statistically significant elevation was absent except for CPA, which showed an increase after 28 days of repeated administration, but its absolute value was quite low (Figure 5). In general, most drugs that had high PC1 values showed high serum concentration of TBIL and DBIL. As shown in Figure 7, the PC1 value had a high correlation with TBIL and DBIL levels.

Possibility of the distinction by samples taken at 24 h after single dose

The above results clearly suggested that the list of extracted 59 probe sets was a useful diagnostic marker for the elevation of TBIL and DBIL in rat liver. The next question is whether the list works as a prognostic marker for drugs elevating TBIL and DBIL. To examine this possibility, we analyzed the data within 24 h of a single dose of the first seven drugs. Figure 8 shows TBIL and DBIL at 3, 6, 9, and 24 h after a single dose. Although there was some significant increase in these measures, most of them were considered to be toxicologically insignificant based on their absolute values. It was thus concluded that no severe elevation of TBIL and DBIL occurred within 24 h for a single dose. Using the gene expression data at 24 h after dosing, PCA was performed using the 59 probe sets. As shown in Figure 9, all the drugs except RIF and CSA were clearly separated from the control samples in the direction of PC1(contribution rate: 33.9%). Among these, CPZ, which showed low PC1 values in repeated dosing (Figures 4 and 6), was not distant from its control by single dosing. Interestingly, however, an excellent separation was attained when extra-high dose of CPZ was added (Figure 9).

Discussion

Hepatotoxic adverse effects, often indicated by cholestasis, are a main concern in drug development and severe hepatotoxicity may cause a drug to be

Table 2 List of 59 probe sets changed in seven compounds elevating of TBIL and DBIL

Probe ID	*Accession No.*	*Gene title*	*Gene symbol*
Lipid metabolic process			
1368520_at	NM_012737	Apolipoprotein A-IV	Apoa4
1370150_a_at	NM_012703	Thyroid hormone responsive protein	Thrsp
1371615_at	BI279069	Diacylglycerol O-acyltransferase homolog 2 (mouse)	Dgat2
1374440_at	BE098506	Dehydrogenase/reductase (SDR family) member 8	Dhrs8
1387139_at	NM_032082	Hydroxyacid oxidase 2 (long chain)	Hao2
1387508_at	NM_017300	Bile acid-Coenzyme A: amino acid N-acyltransferase	Baat
1390549_at	AA859796	Adiponectin receptor 2	Adipor2
1394112_at	AA945123	Hydroxyacid oxidase 1	Hao1
Transporter			
1368621_at	NM_022960	Aquaporin 9	Aqp9
1369074_at	NM_130748	Solute carrier family 38, member 4	Slc38a4
1379592_at	AI045151	Similar to citrin (predicted)	RGD1565889_predicted
1386960_at	NM_031589	Solute carrier family 37 (glucose-6-phosphate transporter), member 4	Slc37a4
1390591_at	AI169163	Solute carrier family 17 (sodium phosphate), member 3	Slc17a3
1393216_at	BI282044	Solute carrier family 33 (acetyl-CoA transporter), member 1	Slc33a1
1398249_at	NM_053965	Solute carrier family 25 (mitochondrial carnitine/ acylcarnitine translocase), member 20	Slc25a20
Ubiquitin-Proteasome			
1383073_at	BG666028	Ubiquitin specific protease 14	Usp14
1398831_at	NM_031629	Proteasome (prosome, macropain) subunit, beta type 4	Psmb4
Mitochondrial function			
1388931_at	AA799440	Mitochondrial ribosomal protein L13	Mrpl13
1367941_at	NM_031326	Transcription factor A, mitochondrial	Tfam
1370918_a_at	BI275939	ATP synthase, H^+ transporting, mitochondrial F1 complex, γpolypeptide 1	Atp5c1
1372080_at	BI287936	Inner membrane protein, mitochondrial	Immt
1398326_at	BI282332	Similar to Nur77 downstream protein 2	MGC105647
Cell proliferation/Cell cycle			
1367764_at	NM_012923	Cyclin G1	Ccng1
1367927_at	BI282863	Prohibitin	Phb
1369738_s_at	NM_017334	cAMP responsive element modulator	Crem
1387714_at	AB031423	cAMP responsive element modulator	Crem
1372437_at	BM390921	S-phase kinase-associated protein 1A	Skp1a
1367512_at	AA998435	Chromatin modifying protein 5	Chmp5
1374591_at	AI409042	similar to protein tyrosine phosphatase, receptor type, D (predicted)	RGD1561090_predicted
1388469_at	AA945615	Insulin-like growth factor I mRNA, 3' end of mRNA	—
Translation			
1367610_at	NM_031103	Ribosomal protein L19	Rpl19
1388244_s_at	BG153272	Ribosomal protein SA	Rpsa
1371973_at	AI237620	Eukaryotic translation initiation factor 3, subunit 6	Eif3s6
Metabolism			
1371076_at	AI454613	Cytochrome P450, family 2, subfamily b, polypeptide 15 /// Cytochrome P450, family 2, subfamily b, polypeptide 2	Cyp2b15 /// Cyp2b2
1368905_at	NM_133586	Carboxylesterase 2 (intestine, liver)	Ces2
1369558_at	NM_022614	Inhibin beta C	Inhbc
1387022_at	NM_022407	Aldehyde dehydrogenase family 1, member A1	Aldh1a1
1387034_at	NM_012619	Phenylalanine hydroxylase	Pah
1388788_at	BG664131	Glutaryl-Coenzyme A dehydrogenase (predicted)	Gcdh_predicted
1398286_at	M64755	Cysteine sulfinic acid decarboxylase	Csad
Response to oxidative stress			
1367896_at	AB030829	Carbonic anhydrase 3	Ca3
1370064_at	AB004454	Presenilin 2	Psen2
Inflammatory response			
1367804_at	NM_017170	Serum amyloid P-component	Apcs
Blood coagulation			
1388330_at	BM384958	Vitamin K epoxide reductase complex, subunit 1	Vkorc1
1374765_at	BI288055	Transcribed locus, moderately similar to XP_001090810.1 fibrinogen gamma chain isoform 9 [Macaca mulatta]	—
Other			
1372479_at	AI175666	Transcribed locus	—
1373313_at	BM391570	Transcribed locus	—
1374943_at	AI170809	Transcribed locus	—
1375845_at	BI290029	Similar to Aig1 protein (predicted)	RGD1562920_predicted
1377048_at	H31813	Similar to cDNA sequence BC021917	RGD1311026

(continued)

Table 2 *(continued)*

Probe ID	*Accession No.*	*Gene title*	*Gene symbol*
1377686_at	AA859337	Transcribed locus	—
1381574_at	BF403907	Similar to putative protein, with at least 6 transmembrane domains, of ancient origin (58.5 kD) (3N884) (predicted)	RGD1312038_predicted
1383732_at	AA819810	Similar to hypothetical protein MGC37914 (predicted)	RGD1307603_predicted
1387856_at	BI274457	Calponin 3, acidic	Cnn3
1388119_at	BM392140	Similar to heterogeneous nuclear ribonucleoprotein A3 /// similar to heterogeneous nuclear ribonucleoprotein A3 (predicted) /// similar to regulator of G-protein signalling like 1	LOC364506 /// LOC684137 /// RGD1566284_predicted
1390326_at	BF564217	Angiogenin, ribonuclease A family, member 1	Ang1
1392172_at	AI169984	Chemokine (C-C motif) ligand 9	Ccl9
1393123_at	BM392153	Complement component 8, gamma polypeptide (predicted)	C8g_predicted
1398409_at	AA850428	Transcribed locus	—

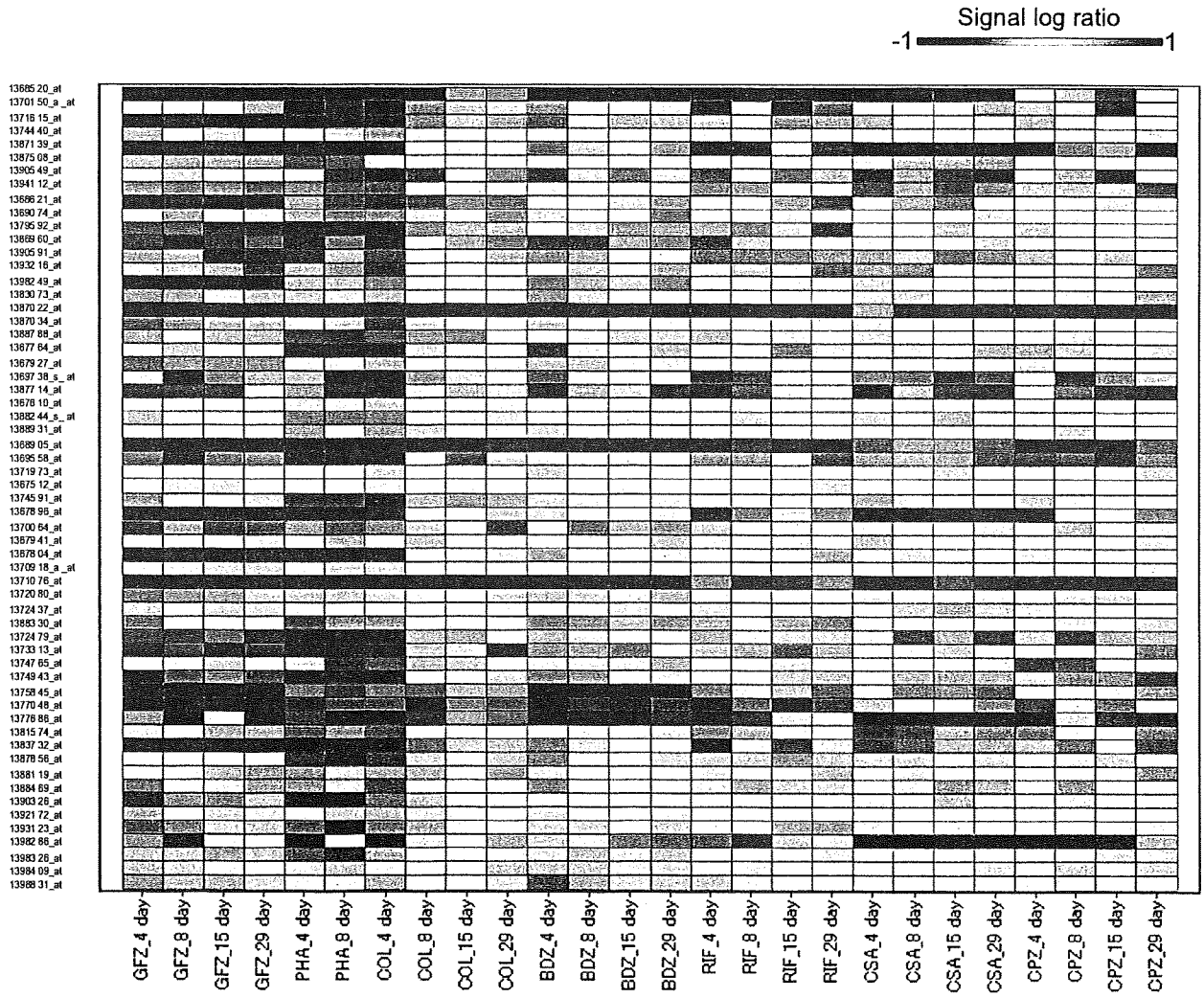

Figure 2 Heat map of the gene expression profiles of gemfibrozil (GFZ), phalloidin (PHA), colchicine (COL), bendazac (BDZ), rifampicin (RIF), cyclosporine A (CSA), and chlorpromazine (CPZ) that induced elevation of total bilirubin (TBIL) and direct bilirubin (DBIL) in the present study using the commonly mobilized 59 probe sets. Values are expressed as average log 2 ratio, for each time point at high dosage.

Table 3 GO analysis of identified 59 probe sets

Term	*Count*	*Percent*	P-*value*
Metabolism	32	51.6	3.5E-3
Cellular metabolism	29	46.8	1.2E-2
Biosynthesis	9	14.5	6.0E-2
Lipid metabolism	6	9.7	6.3E-2
Cellular biosynthesis	8	12.9	8.6E-2
Cellular physiological process	40	64.5	8.8E-2
Response to stress	8	12.9	8.9E-2
Physiological process	43	69.4	9.6E-2
Serine family amino acid metabolism	2	3.2	1.0E-1

withdrawn from the market. Cholestasis results either from a functional defect in bile formation at the level of the hepatocyte (hepatocellular cholestasis) or from an impairment in bile secretion and flow at the level of bile ductules or ducts (ductular/ductal cholestasis). Cholestatic hepatitis is the most common type of drug-induced cholestasis and is more frequent than cholestatic viral hepatitis. It is caused by a metabolic or, more frequently, immunological idiosyncrasy of a drug. Therefore, drugs causing this type of reaction are unpredictable, dose-independent hepatotoxins, and cholestasis occurs only in a small proportion of exposed individuals.

Prototypic drugs causing cholestatic hepatitis include RIF,[8] CPZ,[9–12] GFZ,[13] COL,[14–16] BDZ,[17] CSA,[18–20] and PHA.[21] Indeed, they had elevated TBIL and/or DBIL in our database. We then selected this phenotype to search for a biomarker.

The goal of our project is to extract toxicity biomarkers useful for drug development from our transcriptome database. In the course of our study, we have used a strategy to select a few genes that showed a common change in response to a certain phenotype among the database, but usually we got nothing. Even if we got a candidate, its reproducibility was poor and thus useless. We also frequently experienced such a case that the fingerprint marker genes reported from other institutes are quite different from those in our gene list. This might not be due to the problem of genomics technology, but due to the biology, that is a toxicological phenotype is a result of various biological factors, each of which contains inevitable variations. Therefore, one has to use a strategy to make a prediction based on a pattern of changes of considerable numbers of genes, in order to assure the robustness of the result.

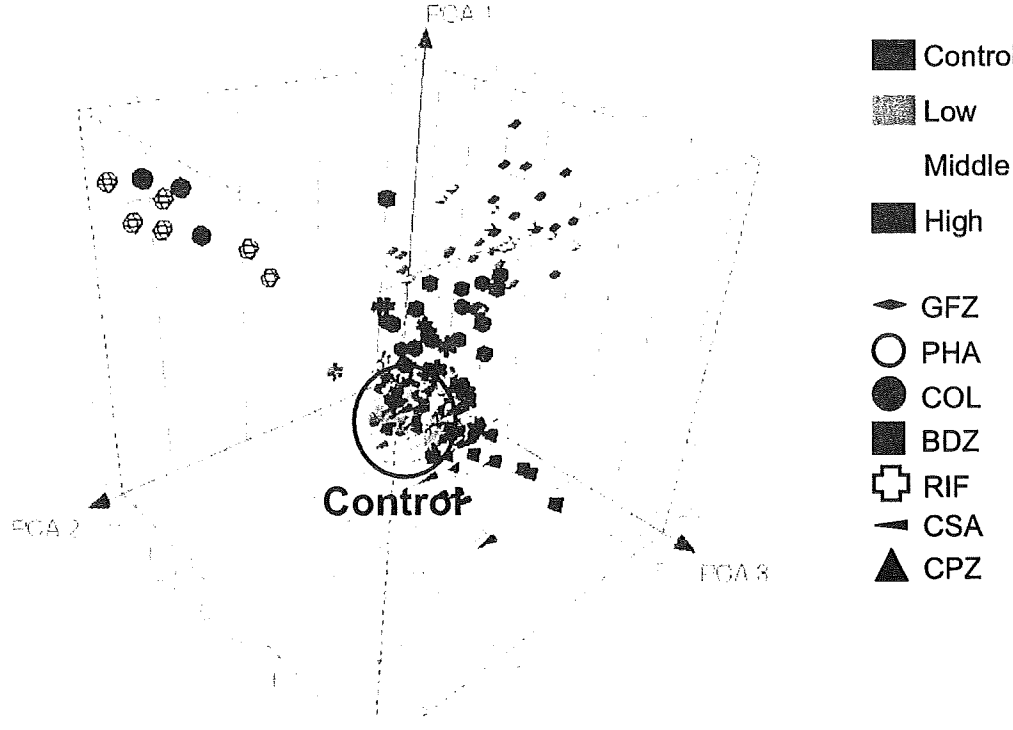

Figure 3 Principal component analysis of the gene expression profiles of gemfibrozil (GFZ), phalloidin (PHA), colchicine (COL), bendazac (BDZ), rifampicin (RIF), cyclosporine A (CSA), and chlorpromazine (CPZ), using the commonly mobilized 59 probe sets. Results are expressed as a three dimensional figure for PC1, 2 and 3. Treated samples were dose-dependently separated from the cluster of the controls (circled by a blue line), mainly toward the direction of PC1 (contribution rate: 30.4 %). For simplicity, rats receiving the same dose with different durations (3, 7, 14, and 28 days [except PHA for 3 and 7 days], $N = 3$ for each; 12 total) are expressed by the same symbol.

Table 4 List of 18 probe sets contributing PC1

Ranking	*Probe set ID*	*Gene title*	*Eigenvalue*
1	1367927_at	Prohibitin	0.202260
2	1368905_at	Carboxylesterase 2 (intestine, liver)	0.197374
3	1387022_at	Aldehyde dehydrogenase family 1, member A1	0.184622
4	1372080_at	Inner membrane protein, mitochondrial	0.183434
5	1375845_at	Similar to Aig1 protein (predicted)	0.180442
6	1398831_at	Proteasome (prosome, macropain) subunit, beta type 4	0.175160
7	1383073_at	Ubiquitin specific protease 14	0.175074
8	1398249_at	Solute carrier family 25 (mitochondrial carnitine/acylcarnitine translocase), member 20	0.170555
9	1372479_at	Transcribed locus	0.154284
10	1398409_at	Transcribed locus	0.143625
11	1372437_at	S-phase kinase-associated protein 1A	0.129215
12	1367512_at	Chromatin modifying protein 5	0.121613
13	1367764_at	Cyclin G1	0.120058
14	1388244_s_at	Ribosomal protein SA	0.118388
15	1367610_at	Ribosomal protein L19	0.116662
16	1371973_at	Eukaryotic translation initiation factor 3, subunit 6	0.110324
17	1388931_at	Mitochondrial ribosomal protein L13	0.109371
18	1367941_at	Transcription factor A, mitochondrial	0.107880

There are two representative ways of classification, that is supervised and unsupervised ones. When the mechanism of action of the drug is clear, or the feature of the drug is undoubtedly designated, a supervised method, such as discriminant analysis is a powerful tool. In fact, we reported a success using this strategy.[3] However, in most of the cases of toxicological phenotypes, it is usually difficult to judge which one is positive or negative. In case of medicines, it hardly happens that a drug never causes a certain phenotype at any dose level. Otherwise, a drug developer needs to know a safety margin. In such cases, it is quite difficult to set positive/negative since the sensitivity of the detection is usually different between gene expression and toxicological phenotype. To our experience, discriminant analysis is often difficult for a phenotype induced by multiple causes or it is highly dependent on the dose level and time after dosing, since a small difference in a choice of positive/negative significantly affects the results. However, unsupervised classification such as PCA or hierarchical clustering enables one to visualize the feature of various drugs semi-quantitatively, although it is not quantitative. This could supply important information for drug development. We already reported candidate marker gene sets for diagnosis and prediction of phospholipidosis.[2]

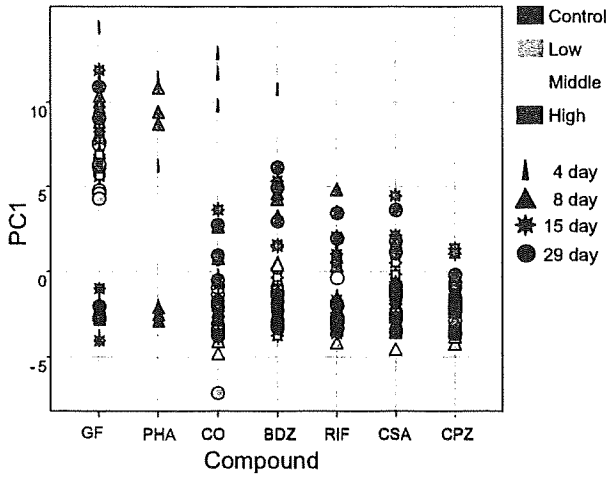

Figure 4 Principal component analysis of the same as Figure 3 but one dimensional expression using principal component 1. For each drug, each individual rat is depicted by a symbol with a different color and shape as shown on the right panel.

In the current study, we used the latter strategy, that is we extracted probe sets for commonly mobilized genes among seven typical drugs causing cholestasis. Using these genes, we have shown that PCA clearly separated dose- and time-dependent clusters of the treated groups from their controls. To verify the usefulness of the probe sets, we explored the potential drugs causing cholestasis in the literature, and further (rarer) examples were found to be antifungal, anthelminthic, antidepressant, anticonvulsive, antihypertensive, antiarrhythmic, antidiabetic, antithyroid, antirheumatic drugs, and H_2-blockers. We then selected 18 drugs for verification from our database.

Of these drugs, MP,[22] TAA,[23] EE,[24–28] ANIT,[29] and PEN[30,31] showed high TBIL and DBIL as well as high PC1 by PCA using these probe sets. In the case of TCP,[32] IM,[33,34] MTS,[35–37] AA,[38] ASA,[39] IPA,[40,41] and INAH,[42] which have been reported to cause cholestasis, these were judged as negative by blood chemical examination in the current study. However, they were clearly separated from their controls by PCA using the probe sets. This suggests that the sensitivity of the diagnosis by gene expression is higher than the measurement of plasma bilirubin.

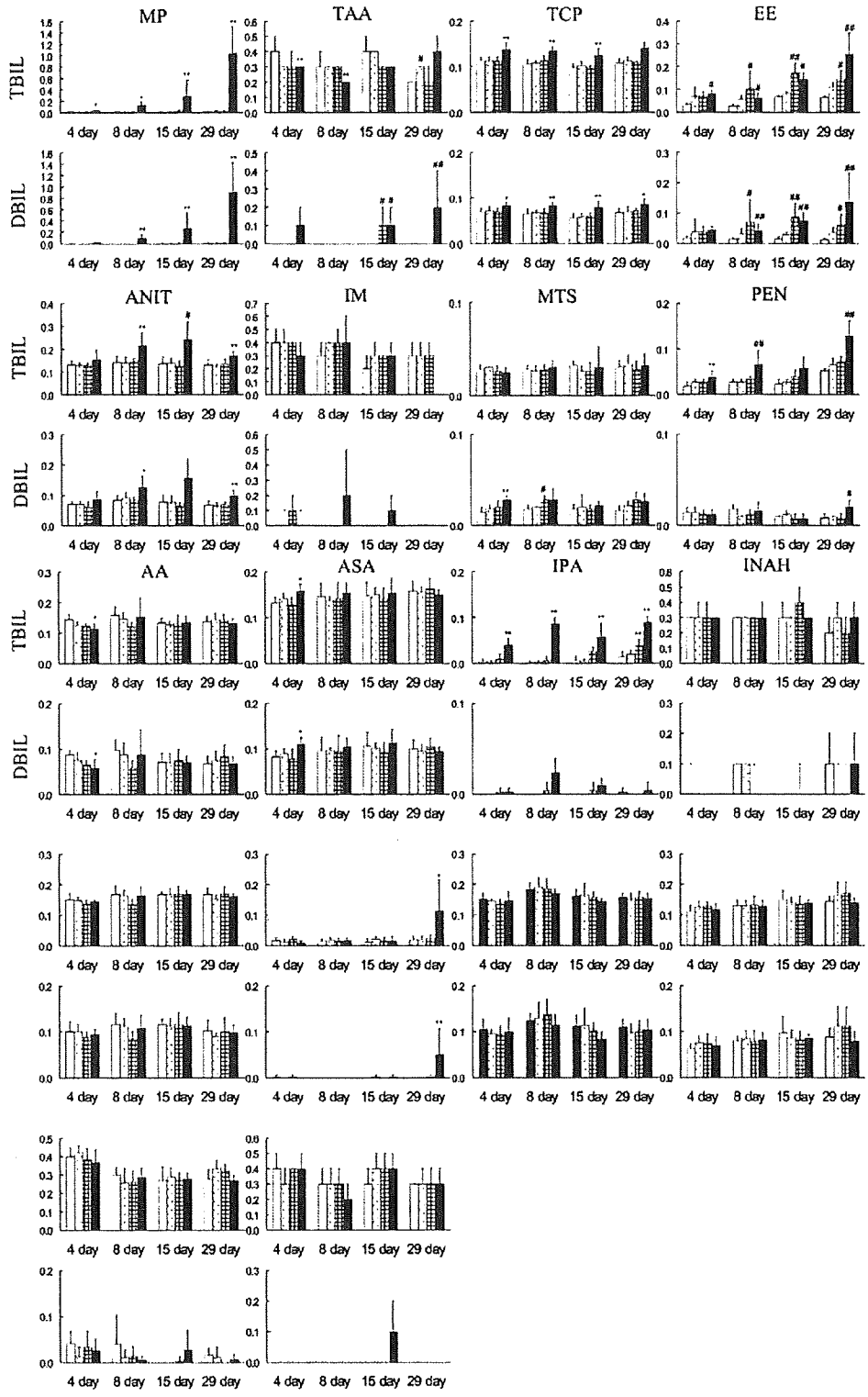

Figure 5 Plasma total bilirubin (TBIL) and direct bilirubin (DBIL) concentrations for rats treated with 18 test-drugs. Plasma TBIL and DBIL concentrations were estimated as shown in Figure 1. Open (control), dotted (low dose), checked (middle dose), and filled (high dose) columns represent plasma TBIL and DBIL concentrations (mg/dL). Values are expressed as mean ± SD of five rats for each time and compound. Significant difference from the control rats: (*$P < 0.05$, **$P < 0.01$: Dunnett test, # $P < 0.05$, ## $P < 0.01$: Dunnett type mean rank test).

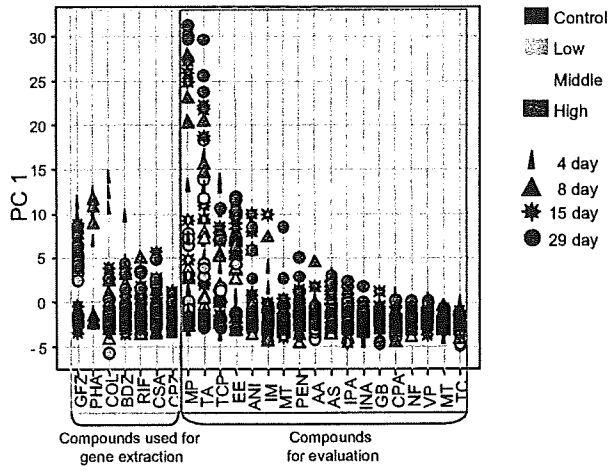

Figure 6 Principal component analysis of gene expression profiles of 18 more drugs which have been reported to elevate total and direct bilirubin, in addition to the seven typical drugs using the commonly mobilized 59 probe sets. Of the 25 compounds, the seven typical compounds used in Figures 3 and 4, are shown on the left panel. Results are expressed as a one dimensional figure with PC1 (contribution rate: 35.9 %). For each drug, each individual rat is depicted by a symbol with a different color and shape, as shown on the right panel.

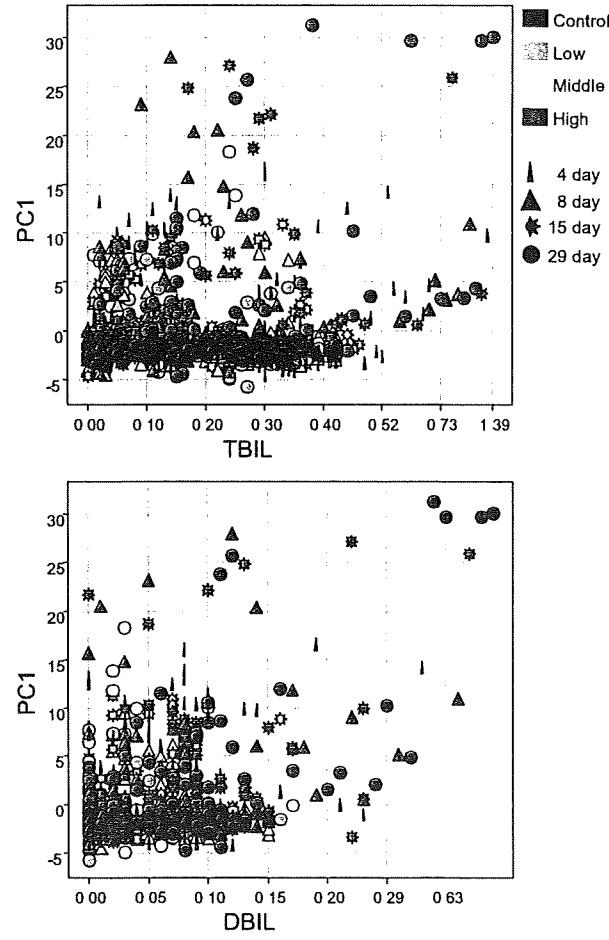

Figure 7 Correlation between the PC1 value, total bilirubin (TBIL), and direct bilirubin (DBIL). Results are expressed as a graph with TBIL or DBIL on the *y*-axis and PC1 value on the *x*. Each individual rat is depicted by a symbol with a different color and shape, as shown on the right panel. Note that the PC1 value shows a high correlation with the TBIL and DBIL with a few exceptions.

CPA is reported to induce cholestasis,[43] but showed a low PC1 value in the current study. Stone, *et al.*[44] observed that plasma bile salt concentration was increased in rats after administration of 10 mg/kg of CPA. They suggested that CPA inhibits the uptake of bile acids from the portal blood into hepatocytes. Moreover, there was no change in liver histology in cholestasis caused by CPA,[45] suggesting that the cytotoxicity of intracellular bile acids induced by CPA is not very severe, and it might be the reason why this drug was not separated by PCA in the current study.

Based on the successful classification of the drugs by PCA using the extracted 59 probe sets, it is expected that the expression changes of these genes are directly or indirectly related to the pathogenesis of cholestasis. From experimental models of cholestasis, several mechanisms have been postulated to account for impaired bile secretion. They are 1) inhibition of Na^+, K^+-ATPase; 2) increased paracellular permeability and regurgitation into plasma of bile constituents; 3) impaired function of the cytoskeleton, mainly microfilaments; 4) alteration of intracellular calcium homeostasis; 5) alteration or mislocation of canalicular carriers; 6) ductular obstruction.[46–48] Reviewing the 59 probe sets, however, we could not identify genes related to the mechanisms listed above. It could be pointed out that it contains considerable numbers of 1) components regulating lipid metabolism, 2) transporters, 3) ubiquitin-proteasome related factors, and 4) mitochondrial components (Table 2).

The discovery that lithocholic acid (LCA) is an endogenous ligand for pregnane X receptor (PXR) suggests that bile acids may also regulate drug metabolism in the liver and intestine by the induction of CYP450 enzymes.[49,50] PXR and its human ortholog steroid and xenobiotic receptor induce the CYP3A, CYP2B, and CYP2C families of steroid- and drug-metabolizing enzymes in the liver and intestine.[51] LCA is the most efficacious bile acid that activates PXR and induces CYP3A4 to catalyze 6-hydroxylation of LCA to hyodeoxycholic acid.[49,50] Lipid metabolic process related genes and CYP2B were generally down-regulated by administration of

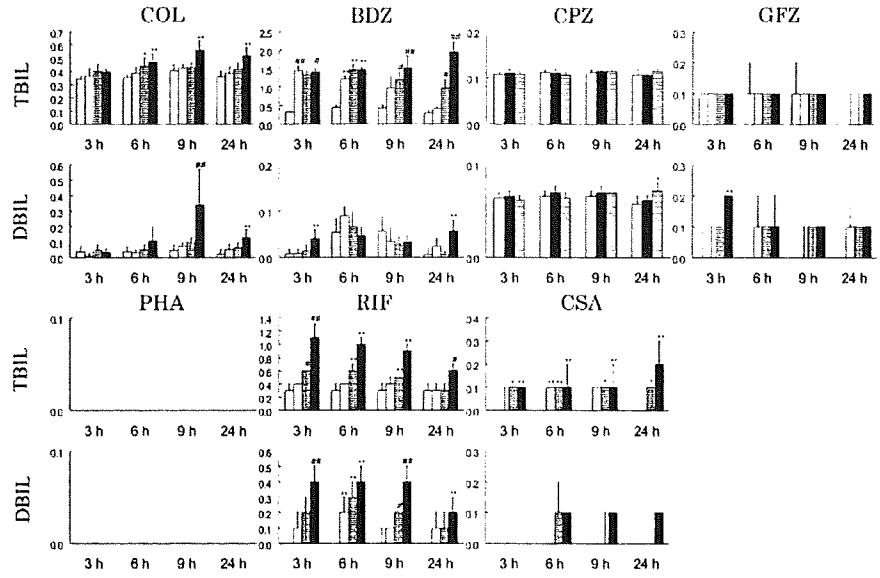

Figure 8 Plasma total bilirubin (TBIL) and direct bilirubin (DBIL) concentrations for rats after a single dose treatment with gemfibrozil (GFZ), phalloidin (PHA), colchicine (COL), bendazac (BDZ), rifampicin (RIF), cyclosporine A (CSA), and chlorpromazine (CPZ). Plasma TBIL and DBIL concentrations were estimated as shown in Figure 1. Open (control), dotted (low dose), checked (middle dose), filled (high dose), and horizontal-striped (extra-high dose) columns represent the plasma TBIL and DBIL concentrations (mg/dL). Values are expressed as mean ± SD of five rats each for each time and compound. Significant difference from the control rats: (*$P < 0.05$, ** $P < 0.01$: Dunnett test, # $P < 0.05$, ## $P < 0.01$: Dunnett type mean rank test). Note that no pathologically meaningful elevation of TBIL and DBIL occurred yet, except for COL, BDZ, and RIF.

the positive drugs in this study. This might be a feedback response to elevated bilirubin.

Hepatic uptake and efflux processes involved in bile formation are maintained by distinct transport systems (sodium-dependent and sodium-independent transport pathways and ATP-dependent efflux pumps) expressed at the two polar surface domains of liver cells.[47] In the current study, some transporters, Aqp9, and Slc families, were mobilized by administration of the drugs causing cholestasis. This might be also a feedback response to elevated bilirubin.

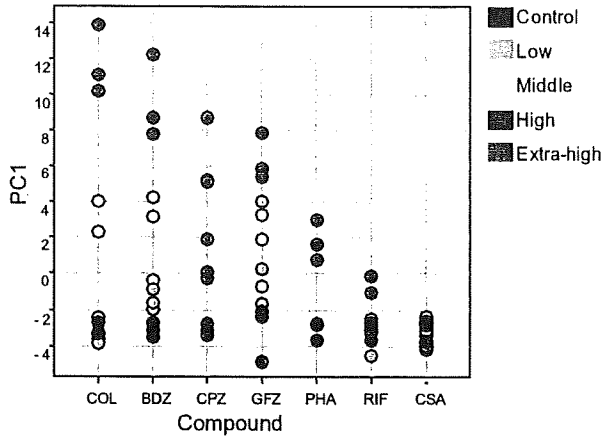

Figure 9 Principal component analysis of gene expression profiles of the samples of 24 h after single dosage using 59 probe sets. Results are expressed as a one dimensional figure with PC1 (contribution rate: 33.9 %). Each individual rat is depicted by a symbol with a different color and shape as shown on the right panel. Note that the higher dose (magenta) showed even higher PC1 values.

At present, we cannot propose a close link between cholestasis and ubiquitin-proteasome or mitochondrial function. For the former, it was reported that ubiquitination of cytokeratin was involved in cholestasis produced by bile-duct ligation.[52] As for the mitochondrial function, it was described that cholestasis practically disturbed mitochondrial bioenergetics,[53] and bile acids were involved in the process of cell death through mitochondrial function.[54] Investigation of these factors in cholestasis would bring a new insight in the understanding of its pathogenesis. For this purpose, the gene list in the current study would supply important information.

In conclusion, we identified 59 probe sets from gene expression profiles in rat liver treated with various bilirubin-elevating compounds stored in our database. PCA using these 59 probe sets would be useful for GeneChip users to predict the risk of cholestasis in the preclinical stage of drug development. At present, it would be difficult to make an appropriate prediction by measuring these genes by another platform, such as quantitative PCR, since the procedure is

dependent on the device. However, it would be possible that these probe sets contain a biomarker(s) useful even in a clinical field. Further work is obviously necessary to improve and generalize the candidate for a marker suggested in this study.

Acknowledgment

This work was supported in part by the grants from Ministry of Health, Labour and Welfare of Japan (H14-Toxico-001 and H19-Toxico-001).

References

1 Urushidani, T. Prediction of hepatotoxicity based on the toxicogenomics database. In: Sahu, SC, (ed), Hepatotoxicity: from Genomics to in vitro and in vivo Models. John Wiley & Sons; 2008. p. 507–529.
2 Hirode, M, Ono, A, Miyagishima, T, Nagao, T, Ohno, Y, Urushidani, T. Gene expression profiling in rat liver treated with compounds inducing phospholipidosis. *Toxicol Appl Pharmacol* 2008; **229**: 290–299.
3 Uehara, T, Hirode, M, Ono, A, Kiyosawa, N, Omura, K, Shimizu, T, *et al.* A toxicogenomics approach for early assessment of potential non-genotoxic hepatocarcinogenicity of chemicals in rats. *Toxicology* 2008; **250**: 15–26.
4 Kiyosawa, N, Uehara, T, Gao, W, Omura, K, Hirode, M, Shimizu, T, *et al.* Identification of glutathione depletion-responsive genes using phorone-treated rat liver. *J Toxicol Sci* 2007; **32**: 469–486.
5 Omura, K, Kiyosawa, N, Uehara, T, Hirode, M, Shimizu, T, Miyagishima, T, *et al.* Gene expression profiling of rat liver treated with serum triglyceride-decreasing compounds. *J Toxicol. Sci.* 2007; **32**: 387–399.
6 Takashima, K, Mizukawa, Y, Morishita, K, Okuyama, M, Kasahara, T, Toritsuka, N, *et al.* Effect of the difference in vehicles on gene expression in the rat liver–analysis of the control data in the Toxicogenomics Project Database. *Life Sci* 2006; **78**: 2787–2896.
7 Dennis Jr, G, Sherman, BT, Hosack, DA, Yang, J, Gao, W, Lane, HC, *et al.* DAVID: Database for annotation, visualization, and integrated discovery. *Genome Biol* 2003; **4**: 3.
8 Adachi, Y, Nanno, T, Yamashita, M, Ueshima, S, Yamamoto, T. Induction of rat liver bilirubin-conjugating enzymes and glutathione S-transferase by rifampicin. *Gastroenterol Jpn* 1985; **20**: 104–110.
9 Knodell, RG. Effects of chlorpromazine on bilirubin metabolism and biliary secretion in the rat. *Gastroenterology* 1975; **69**: 965–972.
10 Mullock, BM, Hall, DE, Shaw, LJ, Hinton, RH. Immune responses to chlorpromazine in rats. Detection and relation to hepatotoxicity. *Biochem Pharmacol* 1983; **32**: 2733–2738.
11 Obata, T. Intrahepatic cholestasis and hyperbilirubinemia in ethynyl estradiol and chlorpromazine-treated rats. *Gastroenterol Jpn* 1983; **18**: 538–548.
12 Ros, E, Small, DM, Carey, MC. Effects of chlorpromazine hydrochloride on bile salt synthesis, bile formation and biliary lipid secretion in the rhesus monkey: a model for chlorpromazine-induced cholestasis. *Eur J Clin Invest* 1979; **9**: 29–41.
13 Jacobs, WH. Intrahepatic cholestasis following the use of Atromid-S. *Am J Gastroenterol* 1976; **66**: 69–71.
14 Barnwell, SG, Lowe, PJ, Coleman, R. The effects of colchicine on secretion into bile of bile salts, phospholipids, cholesterol and plasma membrane enzymes: bile salts are secreted unaccompanied by phospholipids and cholesterol. *Biochem J* 1984; **220**: 723–731.
15 Gregory, DH, Vlahcevic, ZR, Prugh, MF, Swell, L. Mechanism of secretion of biliary lipids: role of a microtubular system in hepatocellular transport of biliary lipids in the rat. *Gastroenterology* 1978; **74**: 93–100.
16 Lowe, PJ, Barnwell, SG, Coleman, R. Rapid kinetic analysis of the bile-salt-dependent secretion of phospholipid, cholesterol and a plasma-membrane enzyme into bile. *Biochem J* 1984; **222**: 631–637.
17 Prieto de Paula, JM, Rodríguez Rodríguez, E, Villamandos Nicás, V, Sanz de la Fuente, H, Prada Mínguez, A, del Portillo Rubí, A. Bendazac hepatotoxicity: analysis of 16 cases. *Rev Clin Esp* 1995; **195**: 387–389.
18 Bramow, S, Ott, P, Thomsen Nielsen, F, Bangert, K, Tygstrup, N, Dalhoff, K. Cholestasis and regulation of genes related to drug metabolism and biliary transport in rat liver following treatment with cyclosporine A and sirolimus (Rapamycin). *Pharmacol Toxicol* 2001; **89**: 133–139.
19 Galan, AI, Zapata, AJ, Roman, ID, Muñoz, ME, Muriel, C, Gonzalez, J, *et al.* Impairment of maximal bilirubin secretion by cyclosporin A in the rat. *Arch Int Physiol Biochim Biophys* 1991; **99**: 373–376.
20 Galán, AI, Fernández, E, Morán, D, Muñoz, ME, Jiménez, R. Cyclosporine A hepatotoxicity: effect of prolonged treatment with cyclosporine on biliary lipid secretion in the rat. *Clin Exp Pharmacol Physiol* 1995; **22**: 260–265.
21 Ishizaki, K, Kinbara, S, Miyazawa, N, Takeuchi, Y, Hirabayashi, N, Kasai, H, *et al.* The biochemical studies on phalloidin-induced cholestasis in rats. *Toxicol Lett* 1997; **90**: 29–34.
22 Steinmetz, KL, Tyson, CK, Meierhenry, EF, Spalding, JW, Mirsalis, JC. Examination of genotoxicity, toxicity and morphologic alterations in hepatocytes following in vivo or in vitro exposure to methapyrilene. *Carcinogenesis* 1988; **9**: 959–963.
23 Martin-Sanz, P, Cascales, C, Gómez, A, Brindley, DN, Cascales, M. Effect of a rhodium complex on alterations of hepatic function in thioacetamide-induced hyperplastic noduligenesis in rats. *Carcinogenesis* 1987; **8**: 1685–1690.
24 Accanito, L, Figuerora, C, Pirazzo, M, Solis, N. Enhanced biliary excretion of canalicular membrane enzymes in estradiol-induced and obstructive cholestasis, and effects of different bile acids in the isolated perfused rat liver. *J Hepatol* 1995; **22**: 658–670.
25 Accanito, L, Pirazzo, M, Solis, N, Koenig, CS, Vollrath, V, Chianale, J. Modulation of hepatic content and biliary excretion of P-glycoproteins in hepatocellular and obstructive cholestasis in the rat. *J Hepatol* 1996; **25**: 349–361.

26 Frezza, M, Tritapepe, R, Pozzato, G, Di Padova, C. Prevention of S-adenosylmethionine of estrogen-induced hepatobiliary toxicity in susceptible women. *Am J Gastroenterol* 1988; **83**: 1098–1102.
27 Sánchez Pozzi, EJ, Crozenci, FA, Pellegrino, JM, Catania, VA, Luquita, MG, Roma, MG, *et al.* Ursodeoxycholate reduces ethinylestradiol glucuronidation in the rat: role of prevention in estrogen-induced cholestasis. *J Pharmacol Exp Ther* 2003; **306**: 279–286.
28 Simon, FR, Fortune, J, Iwahashi, M, Gartung, C, Wolkoff, A, Sutherland, E. Ethinyl estradiol cholestasis involves alterations in expression of liver sinusoidal transporters. *Am J Physiol* 1996; **271**: G1043–G1052.
29 Leonard, TB, Popp, JA, Graichen, ME, Dent, JG. alpha-Naphthylisothiocyanate induced alterations in hepatic drug metabolizing enzymes and liver morphology: implications concerning anticarcinogenesis. *Carcinogenesis* 1981; **2**: 473–482.
30 Barzilai, D, Dickstein, G, Enat, R, Bassan, H, Lichtig, C, Gellei, B. Cholestatic jaundice caused by D-penicillamine. *Ann Rheum Dis* 1978; **37**: 98–100.
31 McLeod, BD, Kinsella, TD. Cholestasis associated with d-penicillamine therapy for rheumatoid arthritis. *Can Med Assoc J* 1979; **120**: 965–966.
32 Wegmann, C, Münzenmaier, R, Dormann, AJ, Huchzermeyer, H. Ticlopidine-induced acute cholestatic hepatitis. *Dtsch Med Wochenschr* 1998; **123**: 146–150.
33 Cappell, MS, Kozicky, O, Competiello, LS. Indomethacin associated cholestasis. *J Clin Gastroenterol* 1988; **10**: 445–447.
34 Martines, G, Boiardi, L, Butturini, L, Bernardi, S, Gelmini, G. Hepatic alterations in indomethacin-treated rabbits. *Clin Rheumatol* 1988; **7**: 24–27.
35 Borhan-Manesh, F, Farnum, JB. Methyltestosterone-induced cholestasis. The importance of disproportionately low serum alkaline phosphatase level. *Arch Intern Med* 1989; **149**: 2127–2129.
36 Tennant, BC, Balazs, T, Baldwin, BH, Hornbuckle, WE, Castleman, WL, Boelsterli, U, *et al.* Assessment of hepatic function in rabbits with steroid-induced cholestatic liver injury. *Fundam Appl Toxicol* 1981; **1**: 329–333.
37 Westaby, D, Ogle, SJ, Paradinas, FJ, Randell, JB, Murray-Lyon, IM. Liver damage from long-term methyltestosterone. *Lancet* 1977; **2**: 262–263.
38 Sell, S. Comparison of liver progenitor cells in human atypical ductular reactions with those seen in experimental models of liver injury. *Hepatology* 1998; **27**: 317–331.
39 López-Morante, AJ, Sáez-Royuela, F, Díez-Sánchez, V, Martín-Lorente, JL, Yuguero, L, Ojeda, C. Aspirin-induced cholestatic hepatitis. *J Clin Gastroenterol* 1993; **16**: 270–272.
40 Nelson, SD, Mitchell, JR, Snodgrass, WR, Timbrell, JA. Hepatotoxicity and metabolism of iproniazid and isopropylhydrazine. *J Pharmacol Exp Ther* 1978; **206**: 574–585.
41 Rosenblum, LE, Korn, RJ, Zimmerman, HJ. Hepatocellular jaundice as a complication of iproniazid therapy. *Arch Intern Med* 1960; **105**: 583–593.
42 Tasduq, SA, Kaiser, P, Sharma, SC, Johri, RK. Potentiation of isoniazid-induced liver toxicity by rifampicin in a combinational therapy of antitubercular drugs (rifampicin, isoniazid and pyrazinamide) in Wistar rats: a toxicity profile study. *Hepatol Res* 2007; **37**: 845–853.
43 Senthilkumar, S, Devaki, T, Manohar, BM, Babu, MS. Effect of squalene on cyclophosphamide-induced toxicity. *Clin Chim Acta* 2006; **364**: 335–342.
44 Stone, BG, Udani, M, Sanghvi, A, Warty, V, Plocki, K, Bedetti, CD, *et al.* Cyclosporin A-induced cholestasis. The mechanism in a rat model. *Gastroenterology* 1987; **93**: 344–351.
45 Kukongviriyapan, V, Stacey, NH. Chemical-induced interference with hepatocellular transport. Role in cholestasis. *Chem-Biol Interact* 1991; **77**: 245–261.
46 Arrese, M, Ananthanarayanan, M. The bile salt export pump: molecular properties, function and regulation. *Pflugers Arch* 2004; **449**: 123–131.
47 Pauli-Magnus, C, Meier, PJ. Hepatobiliary transporters and drug-induced cholestasis. *Hepatology* 2006; **44**: 778–787.
48 Roma, MG, Crocenzi, FA, Sánchez Pozzi, EA. Hepatocellular transport in acquired cholestasis: new insights into functional, regulatory and therapeutic aspects. *Clin Sci (Lond)* 2008; **114**: 567–588.
49 Staudinger, JL, Goodwin, B, Jones, SA, Hawkins-Brown, D, MacKenzie, KI, LaTour, A, *et al.* The nuclear receptor PXR is a lithocholic acid sensor that protects against liver toxicity. *Proc Natl Acad Sci U S A* 2001; **98**: 3369–3374.
50 Xie, W, Radominska-Pandya, A, Shi, Y, Simon, CM, Nelson, MC, Ong, ES, *et al.* An essential role for nuclear receptors SXR/PXR in detoxification of cholestatic bile acids. *Proc Natl Acad Sci U S A* 2001; **98**: 3375–3380.
51 Kliewer, SA, Goodwin, B, Willson, TM. The nuclear pregnane X receptor: a key regulator of xenobiotic metabolism. *Endocr Rev* 2002; **23**: 687–702.
52 Fickert, P, Trauner, M, Fuchsbichler, A, Stumptner, C, Zatloukal, K, Denk, H. Bile acid-induced Mallory body formation in drug-primed mouse liver. *Am J Pathol* 2002; **161**: 2019–2026.
53 Rolo, AP, Oliveira, PJ, Moreno, AJ, Palmeira, CM. Bile acids affect liver mitochondrial bioenergetics: possible relevance for cholestasis therapy. *Toxicol. Sci.* 2000; **57**: 177–185.
54 Rolo, AP, Palmeira, CM, Holy, JM, Wallace, KB. Role of mitochondrial dysfunction in combined bile acid-induced cytotoxicity: the switch between apoptosis and necrosis. *Toxicol Sci* 2004; **79**: 196–204.

Toxicology 265 (2009) 15–26

Contents lists available at ScienceDirect

Toxicology

journal homepage: www.elsevier.com/locate/toxicol

Identification of genomic biomarkers for concurrent diagnosis of drug-induced renal tubular injury using a large-scale toxicogenomics database

Chiaki Kondo[a,1], Yohsuke Minowa[b,*,1], Takeki Uehara[a,**,1], Yasushi Okuno[c], Noriyuki Nakatsu[b], Atsushi Ono[d], Toshiyuki Maruyama[a], Ikuo Kato[a], Jyoji Yamate[e], Hiroshi Yamada[b], Yasuo Ohno[f], Tetsuro Urushidani[b,g]

[a] Developmental Research Laboratories, Shionogi & Co., Ltd., 3-1-1, Futaba-cho, Toyonaka, Osaka, Japan
[b] Toxicogenomics-Informatics Project, National Institute of Biomedical Innovation, 7-6-8 Asagi, Ibaraki, Osaka 567-0085, Japan
[c] Department of Systems Bioscience for Drug Discovery, Graduate School of Pharmaceutical Sciences, Kyoto University, 46-29, Yoshida Shimoadachi-cho, Kyoto 606-8501, Japan
[d] Division of Risk Assessment, National Institute of Health Sciences, Kamiyoga 1-18-1, Setagaya-ku, Tokyo 158-8501, Japan
[e] Department of Veterinary Pathology, Graduate School of Agriculture and Biological Science, Osaka Prefecture University, 1-1 Gakuen- cho, Sakai, Osaka 599-8531, Japan
[f] National Institute of Health Sciences, Kamiyoga 1-18-1, Setagaya-ku, Tokyo 158-8501, Japan
[g] Department of Pathophysiology, Faculty of Pharmaceutical Sciences, Doshisha Women's College of Liberal Arts, Kodo, Kyotanabe, Kyoto 610-0395, Japan

ARTICLE INFO

Article history:
Received 4 August 2009
Received in revised form 3 September 2009
Accepted 4 September 2009
Available online 15 September 2009

Keywords:
Toxicogenomics
Microarray
Biomarkers
Rat
Nephrotoxicity
Necrosis

ABSTRACT

Drug-induced renal tubular injury is one of the major concerns in preclinical safety evaluations. Toxicogenomics is becoming a generally accepted approach for identifying chemicals with potential safety problems. In the present study, we analyzed 33 nephrotoxicants and 8 non-nephrotoxic hepatotoxicants to elucidate time- and dose-dependent global gene expression changes associated with proximal tubular toxicity. The compounds were administered orally or intravenously once daily to male Sprague-Dawley rats. The animals were exposed to four different doses of the compounds, and kidney tissues were collected on days 4, 8, 15, and 29. Gene expression profiles were generated from kidney RNA by using Affymetrix GeneChips and analyzed in conjunction with the histopathological changes. We used the filter-type gene selection algorithm based on *t*-statistics conjugated with the SVM classifier, and achieved a sensitivity of 90% with a selectivity of 90%. Then, 92 genes were extracted as the genomic biomarker candidates that were used to construct the classifier. The gene list contains well-known biomarkers, such as *Kidney injury molecule 1*, *Ceruloplasmin*, *Clusterin*, *Tissue inhibitor of metallopeptidase 1*, and also novel biomarker candidates. Most of the genes involved in tissue remodeling, the immune/inflammatory response, cell adhesion/proliferation/migration, and metabolism were predominantly up-regulated. Down-regulated genes participated in cell adhesion/proliferation/migration, membrane transport, and signal transduction. Our classifier has better prediction accuracy than any of the well-known biomarkers. Therefore, the toxicogenomics approach would be useful for concurrent diagnosis of renal tubular injury.

1. Introduction

Toxicogenomics, which is the application of microarray technologies to toxicology, is becoming a generally accepted approach for identifying chemicals with potential safety problems. Identifying drug safety liabilities or predictive biomarkers for drug-induced organ damage at or before the preclinical stages of drug development is of great importance to pharmaceutical companies. The ability to determine whether or not to pursue the development of a drug based on safety would greatly reduce the cost of drug development and improve the attrition rate of new chemical entities. Currently, preclinical drug safety evaluation relies mainly on complex histopathological or clinical pathological analysis. These traditional approaches have proven to be highly successful but may fail to detect prodromal and early stages of toxicity. Genomic data can be more sensitive and objective than traditional methods for the early prediction of compound-induced toxicity. Microarray expression profiling during preclinical drug development is expected to aid in uncovering unexpected or secondary pharmacology, predicting adverse effects, and understanding the mechanisms of drug action or toxicity (Battershill,

* Corresponding author. Tel.: +81 72 641 9826; fax: +81 72 641 9850.
** Corresponding author. Tel.: +81 6 6331 8195; fax: +81 6 6332 6385.
E-mail addresses: yminowa@nibio.go.jp (Y. Minowa), takeki.uehara@shionogi.co.jp (T. Uehara).
[1] These authors equally contributed to this work.

0300-483X/$ – see front matter © 2009 Elsevier Ireland Ltd. All rights reserved.
doi:10.1016/j.tox.2009.09.003

2005; Heinloth et al., 2004; Irwin et al., 2004; Searfoss et al., 2005).

The kidney is a major organ for the filtration, secretion, re-absorption and ultimately the excretion of drugs or drug metabolites. Nephrotoxicity frequently occurs after administration of various drugs or xenobiotics. The tubular cells of the kidney are particularly vulnerable to drug-induced injury, and thus renal tubular toxicity is a major concern in preclinical safety evaluations. Drug-induced tubular damage has been well documented and extensively studied (Perazella, 2005). The prediction and diagnosis of preclinical renal tubular toxicity based on molecular methods that use microarray gene expression data have been attempted. Fielden et al. (2005) assessed predicative gene expression endpoints at early time points proceeding the onset of any signs of renal tubular pathology, and they achieved a prediction accuracy of 76%. In a separate study that assessed the expression profiling endpoints in parallel with the histopathological diagnosis of concurrent renal tubular toxicity, the performance was improved and a sensitivity of 82% was achieved with 100% of selectivity (Thukral et al., 2005). Furthermore, Jiang et al. (2007) achieved a sensitivity of 88% and a specificity of 91% using the expression profiling endpoints in parallel with the histopathological diagnosis of concurrent renal tubular toxicity. It is thought that concurrent diagnosis is easier than the prediction of future onset because the early stage toxic gene expression changes are heterogenic between different compounds, but the gene expression changes concurrent with the same toxic endpoints are comparatively homogenous among different compounds.

The Toxicogenomics Project (TGP) is a public–private collaborative project of the National Institute of Health Sciences, the National Institute of Biomedical Innovation, and 15 pharmaceutical companies in Japan that began in 2002 (Urushidani and Nagao, 2005). Its aim is to construct a large-scale toxicology database of transcriptomes that are useful to predict the toxicity of new chemical entities in the early stages of drug development. Until now, about 150 chemicals, primarily medicinal compounds, were selected and gene expression profiles of multiple doses and times in the rat liver and kidney, and rat and human hepatocytes were comprehensively analyzed by using the Affymetrix GeneChip® (over 27,000 profiles). These gene expression profiles, conjugated with the histopathological changes, the results of blood biochemical examinations, and the other phenotypic profiles, are stored in our database with a web-based tool for statistical analysis named TG-GATEs (Genomics Assisted Toxicity Evaluation System developed by Toxicogenomics Project in Japan). Thirteen of the 150 chemicals were typical nephrotoxicants or drugs showing clinical side effects (e.g., cisplatin, carboplatin, gentamicin, vancomycin, phenacetin, and bucetin), and 20 chemicals exhibited nephrotoxicity in addition to hepatotoxicity (e.g., phenylbutazone, ethionine, and indomethacin). We measured gene expression profiles in the kidney after exposure to the group of 33 nephrotoxicants and a negative control group of 8 hepatotoxicants; thus, data from 41 chemicals are presently available for the analysis of nephrotoxicity. The specific aim of the present study was to develop identifiers for concurrent diagnosis of drug-induced tubular injury based on gene expression profiles available from our toxicogenomics database.

The possibility that a genomics evaluation could lead to the elucidation of biomarkers that provide additional sensitivity and/or earlier detection of renal tubular damage is intriguing. A biomarker discovery effort requires experimental designs that encompass several compounds of diverse chemical natures that cause the same toxic endpoint. In addition, multiple time points and doses are necessary to tease out the gene expression changes that are early indicators of the severity and progression of lesions. Therefore, it is reasonable to at first elucidate genetic biomarkers for concurrent diagnosis at the same toxic endpoints, because these gene expression profiles are relatively homogenous compared to the profiles at the early stage of toxicity. Moreover, in the examination of sensitive toxicogenomics data, it is necessary to distinguish adverse changes from changes that are normal physiologic adaptive responses within a no observable adverse effect level (NOAEL). Also, when a biomarker is intended for broad research or regulatory use, the size and diversity of the training set must be considered, and validation of the biomarker on external data must be demonstrated (Somorjai et al., 2003; Ransohoff, 2004). A large-scale toxicogenomics database containing data from multiple time points and drug doses is useful to reliably assess hypotheses generated in other studies that have used comparatively small datasets.

In the present analysis, we extracted candidate biomarkers for the concurrent diagnosis of nephrotoxicity using the large-scale microarray dataset generated in our project. The microarray samples treated with nephrotoxicants and hepatotoxicants were divided into positives and negatives of the training set according to their histopathological findings, to perform supervised classification algorithms after selecting differentially expressed genes. We used three different types of algorithms for gene selection and classification to select the most appropriate method for our dataset and the development of statistically robust analysis. The external test sets were randomly generated 100 times by dividing the training set into subsets, and the prediction accuracy was calculated by summarizing the prediction results of the external test sets. As a result, we achieved a sensitivity of 90% with a selectivity of 90%. Then, 92 genes were extracted as the genomic biomarker candidates that were used to construct the classifier. The group of extracted genes contains well-known biomarkers, such as *Kidney injury molecule-1* (*Kim1*), *Ceruloplasmin* (*Cp*), *Clusterin* (*Clu*), *Tissue inhibitor of metallopeptidase 1* (*Timp1*), *Secreted phosphoprotein 1* (*Spp1*), and also novel biomarker candidates. Our multigene-based classifier had better classification accuracy than any of the single well-known biomarkers; therefore, toxicogenomics would be more useful for concurrent diagnosis of renal tubular injury than any of the previous criteria.

2. Materials and methods

2.1. Compounds

The chemical name, abbreviation, dosage, administration route and vehicle for each compound used in this study are summarized in Table 1.

2.2. Animal treatment

Five-week-old male Sprague-Dawley rats were obtained from Charles River Japan, Inc. (Kanagawa, Japan). After a 7-day quarantine and acclimatization period, 6-week-old animals were assigned to dosage groups (five rats per group) using a computerized stratified random grouping method based on individual body weight. The animals were individually housed in stainless-steel cages in an animal room that was lighted for 12 h (7:00–19:00) each day, ventilated with an air-exchange rate of 15 times per hour, and maintained at 21–25 °C with a relative humidity of 40–70%. Each animal was allowed free access to water and pellet diet (CRF-1, sterilized by radiation, Oriental Yeast Co., Ltd., Tokyo, Japan). Rats in each group received orally administered drugs that were suspended or dissolved in 0.5% methylcellulose solution (MC) or corn oil according to their dispersibility, with the exceptions of cisplatin, carboplatin, 2-bromoethylamine, cephalothin, puromycin aminonucleoside, gentamicin, vancomycin and doxorubicin, which were dissolved in saline and administered intravenously. The animals were treated for 3, 7, 14, or 28 days and sacrificed 24 h after the last dose. Blood samples from the abdominal aorta were collected in a heparinized tube after the rats were anesthetized with ether. After collecting the blood, the animals were euthanized by exsanguination from the abdominal aorta. For histopathological examination, kidney samples were fixed in 10% neutral-buffered formalin, dehydrated in alcohol and embedded in paraffin. Paraffin sections were prepared and stained using standard methods for hematoxylin and eosin staining (H&E). The experimental protocols were reviewed and approved by the Ethics Review Committee for Animal Experimentation of the National Institute of Health Sciences.

Table 1
In vivo compound treatments used in training and testing.

Compound	Dose (mg/kg/day; repeated)	Vehicle	Route
Gentamicin sulphate	~100	Saline	iv
Vancomycin hydrochloride	~200	Saline	iv
2-Bromoethylamine hydrobromide	~20	Saline	iv
Phenylbutazone	~200	0.5% MC	po
Cyclosporine A	~100	Corn oil	po
Thioacetamide	~45	0.5% MC	po
K17	~600	0.5% MC	po
Triamterene	~150	0.5% MC	po
Allopurinol	~150	0.5% MC	po
Nitrofurantoin	~100	0.5% MC	po
Ethionine	~250	0.5% MC	po
N-Phenylanthranilic acid	~1000	0.5% MC	po
Cisplatin	~1	Saline	iv
Phenacetin	~1000	0.5% MC	po
Puromycin aminonucleoside	~40	Saline	iv
Lomustine	~6	0.5% MC	po
Cyclophosphamide	~15	0.5% MC	po
Carboplatin	~10	Saline	iv
Hexachlorobenzene	~300	Corn oil	po
Captopril	~1000	0.5% MC	po
Enalapril	~600	0.5% MC	po
Indomethacin	~5	0.5% MC	po
Doxorubicin hydrochloride	~1	Saline	iv
Ethinyl estradiol	~10	Corn oil	po
Monocrotaline	~30	0.5% MC	po
Acetaminophen	~1000	0.5% MC	po
Cephalothin sodium	~2000	Saline	iv
Bucetin	~1000	0.5% MC	po
Methyltestosterone	~300	0.5% MC	po
Rifampicin	~200	0.5% MC	po
Imipramine hydrochloride	~100	0.5% MC	po
Acetazolamide	~600	0.5% MC	po
Caffeine	~100	0.5% MC	po
Valproic acid	~450	0.5% MC	po
Clofibrate	~300	Corn oil	po
Allyl alcohol	~45	Corn oil	po
Omeprazole	~1000	0.5% MC	po
Bromobenzene	~300	Corn oil	po
Ketoconazole	~100	0.5% MC	po
Ciprofloxacin	~1000	0.5% MC	po
Erythromycin ethylsuccinate	~1000	0.5% MC	po

Male SD rats received oral or intravenous doses once daily (6 weeks of age, $n = 5$). Four, 8, 15, and 29 days after the start of repeated administrations, the kidney tissues were collected and used for gene expression analysis (Affymetrix GeneChip®, $n = 3/5$). Four doses were used for each compound including vehicle control (vehicle control, low, middle, high dose level). Different doses were used for single and repeated administration. po: peroral, iv: intravenous.

2.3. Microarray analysis

An aliquot of the tissue sample (whole slice; about 30 mg) for RNA analysis was obtained from the kidney in each animal immediately after sacrifice. Tissue samples were kept in RNAlater® (Ambion, Austin, TX, USA) overnight at 4 °C, and then frozen at −80 °C until use. Kidney samples were homogenized with buffer RLT that was supplied with the RNeasy mini kit (Qiagen, Valencia, CA, USA), and total RNA was isolated according to the manufacturer's instructions. Microarray analysis was conducted on 3 of 5 samples for each group by using GeneChip® Rat Genome 230 2.0 Arrays (Affymetrix, Santa Clara, CA, USA), which contain 31,042 probe sets. The procedure was conducted basically according to the manufacturer's instructions by using One-Cycle Target Labeling and Control Reagents (Affymetrix) for cDNA synthesis, purification, and the synthesis of biotin-labeled cRNA. Ten micrograms of fragmented cRNA was hybridized to a Rat Genome 230 2.0 Array for 18 h at 45 °C at 60 rpm, after which the array was washed and stained with streptavidin-phycoerythrin by using Fluidics Station 400 (Affymetrix) and then scanned with a Gene Array Scanner (Affymetrix). The digital image files were preprocessed by Affymetrix Microarray Suite version 5.0 (MAS5.0) and converted into base10 logarithmic values. Then, these values were normalized into *Z*-scores by using Tukey's biweight algorithm. The normalized datasets were reversed into non-logarithmic values by calculating their exponential numbers in decimal, and the log-ratio of base 2 to the means of the control groups were calculated.

2.4. Gene selection and supervised classification

High-dose groups of 23 compounds that caused necrosis, degeneration, or regeneration in the renal tubules during chronic exposure were defined as the positive set. Low-dose groups of all of 41 compounds and high-dose groups of the eight hepatotoxicants, which had no histopathological findings, were defined as the negative set. Other high-dose groups of 10 compounds and middle-dose groups were treated as the external test set. Both filter-type and wrapper-type gene selection algorithms and Support Vector Machine (SVM; Vapkin, 1995) and Prediction Analysis of Microarrays (PAM; Tibshirani et al., 2002) supervised classification algorithms were used to extract the biomarker candidates and construct classifiers using the selected genes. Recursive feature elimination (SVM-RFE; multivariate type; Guyon et al., 2002) and nearest shrunken centroid (PAM; univariate type) were used as wrapper-type gene selection algorithms, and Intensity-Based Moderated *T*-statistics (IBMT; Sartor et al., 2006) was used as a filter-type gene selection algorithm (SVM was used as the classifier, in this case).

Five-fold cross-validation (CV) was executed for optimization of the classifiers and to calculate their prediction accuracies. At first, the whole positive and negative training datasets were randomly divided into five subsets of roughly equal size. The SVM and PAM were trained with a selection of optimal genes on eight subsets (four positive subsets and four negative subsets) and then applied to the remaining subset as the test dataset. The negative samples of the test subset were randomly excluded to adjust the number to the positive samples before prediction. Before training of the SVM, optimal genes were selected from the training set by using "Recursive Feature Elimination" (SVM-RFE) or "Intensity-Based Moderated *T*-statistics" (SVM+IBMT). One to 99 of the top-ranked genes of each selection strategy were used to construct the classifiers. Also, in the case of the PAM classifier, 3 to 10 were used as the threshold of the centroid shrinkage to select top-ranked genes. The feature genes used in each training set were filtered by MAS5.0 P/A-call (excluded the probes that were judged as absent in all samples of the training set) and fold change (excluded the probes whose absolute $\log_2$ ratio values were less than 1 between the positives and the negatives) during the 5-fold CV, before being selected and ranked by the feature selection algorithms.

The classifiers were also tested by making the external test datasets by randomly dividing 23 compounds containing positive samples and 18 compounds containing

only negative samples into 5 subsets. An arbitrary subset (combining a positive subset and a negative subset) and the remaining subsets were respectively treated as the external test set and the training set. Compounds of the test subset containing only negative samples were randomly excluded to adjust the number of negative samples to the positive samples before prediction. The feature genes were selected from the training set and used to construct the classifier, which was used to predict the external test set. This process was repeated 100 times, and the prediction accuracy was calculated as the sum of all of the prediction results calculated. Then, the whole positive and negative datasets were used to construct the classifier and to predict the external test set (high-dose groups of 10 compounds and middle-dose groups of all of 41 compounds).

3. Results

3.1. Histopathological examination

The results of the histopathological examinations for all compounds are summarized in Table 2. The high-dose groups of 23 tubular toxicants (gentamicin sulphate, vancomycin hydrochloride, 2-bromoethylamine hydrobromide, phenylbutazone, cyclosporine A, thioacetamide, K17, triamterene, allopurinol, nitrofurantoin, ethionine, *N*-phenylanthranilic acid, cisplatin, phenacetin, puromycin aminonucleoside, lomustine, cyclophosphamide, carboplatin, hexachlorobenzene, captopril, enalapril, indomethacin, and doxorubicin hydrochloride) exhibited necrosis, degeneration, and/or regeneration of the renal tubules at one or more sacrifice time during chronic exposure (days 4, 8, 15, and 29). Among them, 10 compounds (gentamicin sulphate, vancomycin hydrochloride, phenylbutazone, cyclosporine A, thioacetamide, K17, triamterene, allopurinol, *N*-phenylanthranilic acid, and cisplatin) exhibited the histopathological findings at all sacrifice time points. Tubular damage caused by nitrofurantoin or ethionine was repaired by day 15 or 29. The other 11 compounds caused nephrotoxicities only after a long period of chronic exposure (2-bromoethylamine hydrobromide, phenacetin, puromycin aminonucleoside after day 8, lomustine after day 15, and cyclophosphamide, carboplatin, hexachlorobenzene, captopril, enalapril, indomethacin, and doxorubicin hydrochloride after day 29). Although 10 of the potential tubular toxicants did not cause necrosis, degeneration, or regeneration, 6 of these 10 compounds caused other histopathological findings, such as vacuolation, anisonucleosis, hyaline droplet, swelling, hypertrophy, eosinophilic body, and cytoplasmic granule.

The middle-dose groups of 14 of the 23 tubular toxicants (gentamicin sulphate, cyclosporine A, thioacetamide, K17, triamterene, allopurinol, nitrofurantoin, ethionine, *N*-phenylanthranilic acid, cisplatin, puromycin aminonucleoside, hexachlorobenzene, captopril, and enalapril) had histopathological findings. Triamterene and allopurinol had histopathological findings at all of the sacrifice time points. The tubular damage in the middle-dose groups of nitrofurantoin and ethionine was repaired after long-time chronic exposure, which is consistent with their high-dose groups. The other 10 compounds yielded histopathological findings only after long-time chronic exposure. Thioacetamide only had histopathological findings at day 15. Although low-dose groups of 19 of the 23 tubular toxicants had no histopathological findings, the low-dose groups of gentamicin sulphate, triamterene, puromycin aminonucleoside, and hexachlorobenzene had degeneration or regeneration in renal tubules and/or cortex. In the case of gentamicin sulphate, triamterene, and hexachlorobenzene, only one or two animals in a group of five animals had minimal/slight degeneration/regeneration in the renal tubules. The animal that had the histopathological findings was not used for the microarray experiment (in the case of triamterene). The low-dose group of puromycin aminonucleoside had slight degeneration ($n = 4/5$) and regeneration ($n = 2/5$) in the renal tubules on day 29. But, the animals did not have apparent necrosis findings or significant changes in BUN/CRE. Therefore, we considered these findings to be negative.

3.2. Microarray data analysis

3.2.1. Gene selection and supervised classification

For statistical reliability and regulatory perspective to determine the most appropriate analytical methods for the large-scale toxicogenomics database, we examined three different types of classification strategies, SVM-RFE, SVM+IBMT, and PAM. As the result of 5-fold cross-validation (randomly divided samples), we achieved the sensitivity of each classifier of 94% (SVM-RFE; 99 probes), 93.8% (SVM+IBMT; 99 probes), and 90% (PAM; threshold = 5.4), when we allowed 10% of false positives (Supplementary figures). Although the SVM-RFE was expected to have the highest classification accuracy, the correspondence rate of the feature gene list selected by recursive feature elimination between the sub-training sets was smaller than for the other two algorithms. The SVM-RFE classifier appeared to be over-fitted to the training set, so that the selected genes were not robust and were inadequate to be used as the biomarkers. In contrast, the feature genes selected by SVM+IBMT and PAM were similar between different training datasets generated during 5-fold CV. The prediction accuracy of the SVM+IBMT classifier was better than the PAM classifier. Therefore, we selected SVM+IBMT as the gene selection and classification algorithm.

We also tested prediction accuracy using the external test set. The group of 23 compounds containing positive samples and the group of 18 compounds containing only negative samples were randomly divided into 5 subsets 100 times. An arbitrary subset was used as the external test set, and the remaining subsets were used as the training set. We summarized the prediction results and achieved a sensitivity of 94.7% (SVM-RFE; 62 probes), 90% (SVM+IBMT; 98 probes), and 85.7% (PAM; threshold = 10) with a selectivity of 90% (Supplementary figures). In all three algorithms, the prediction accuracies calculated by using the external test sets were decreased compared to the accuracies calculated by 5-fold CV randomly divided samples. In the latter case, the training set and the test set possibly shared samples of the same compounds, times, and doses, such that the estimated accuracy was inappropriately high. It is always desirable to calculate the prediction accuracy using an external test set.

We used the top 98 probes (92 genes) to construct the SVM+IBMT classifier, considering the prediction accuracy and to avoid over-fitting (Table 3). The prediction accuracy was almost saturated and not significantly decreased compared to the max value, the number of support vectors was adequately lowered, and the number of feature genes was substantially smaller than the number of samples to avoid over-fitting (Supplementary figures). Also, the feature gene list is long enough to interpret their biological relevance. The probes ranked below the top 98 were also induced in renal tubular injury and biologically relevant. But around the top 600 genes, the number of support vectors was gradually increased, which means that these genes provided no more or little information for classification and tended to be over-fitting. The whole feature genes ranking is provided in the Supplementary Table. In addition, we tested the classifiers constructed from well-established single-genetic biomarkers and found that the classifier constructed from the multiple feature genes had much better prediction accuracy (Supplementary figures).

3.2.2. The gene expression profile of the feature genes

Fig. 1 shows the expression profile of the top 98 probes (92 genes) described above. Each color represents the *Z*-score of the log-ratio to the mean expression value of the corresponding control samples. The *Z*-scores were calculated by dividing the log-ratio